Online oil-in-water and suspended solids measurement device based on thermal lens spectrometry and forward scattering

Axel Lacapmesure[a,*], Darío Kunik[b], Oscar E. Martínez[c]

[a] *Departamento de Física, Facultad de Ciencias Exactas y Naturales, Universidad de Buenos Aires, Ciudad Autónoma de Buenos Aires, Argentina*
[b] *YPF Tecnología S.A., Buenos Aires, Argentina*
[c] *Laboratorio de Fotónica, Facultad de Ingeniería, Universidad de Buenos Aires, Ciudad Autónoma de Buenos Aires, Argentina*

Abstract

Keywords:

Falta:

- Revisar introducción. Copiar referencias de la tesis/patente.
- Abstract y conclusiones.
- Mostrar señal típica (quizás con histograma, moda y dispersión) y detección de picos.
- Traducir figuras, adecuarlas 1 columna (excepto setup). Agregar mediciones corregidas para dilución de IW100 en IW10.
- Serruchar cosas.
- Unificar terminología: "thermal lens channel" vs "thermal lens signal" vs "*FE*"...

1. Introduction

Water quality monitoring is essential for most stages of oil production. In all water injection projects such as secondary oil recovery, maintaining high injectivities over long periods of time is extremely important, but depositions of organic material and suspensions solids from injection water produces well plugging that reduces oil production. In tertiary oil recovery, the manufacturing of polymers for chemical injection typically requires high quality water since the presence of hydrocarbons may trigger the agglomeration of solids which also induce well plugging. Well cleaning demands expensive procedures and suspends oil production, so water quality monitoring is necessary for both prevention and to evaluate water treatment processes. Additionally, controlling water quality is a requirement in offshore oil recovery, where wastewater is usually poured onto the sea and hence strict regional regulations controls its allowed hydrocarbon concentrations.

Water quality analysis can be conducted on field and outside field, and typically comprises taking a sample of the water under study and then detect and measure the concentration of its components by means of diverse procedures that usually involves chemical extraction and/or separation techniques. While these analyses are fundamental since they can provide results in absolute units and allows for comparison of results obtained from different installations, they usually demands long times (as long as several weeks) until results are available and thus are impracticable for process trending and detection of process deviation, which requires online monitors. In the

*Corresponding author
Email address: axel.lacapmesure@gmail.com (Axel Lacapmesure)

last decades, alternative techniques based on optical phenomena were developed and implemented aiming to respond to this need, and they are currently available in the market. Below we briefly discuss the most noteworthy examples.

Scattering based methods detects the angular distribution of light scattered by oil droplets and other suspended particles contained in the sample. These systems don't account for dissolved hydrocarbons and showed difficulties to differentiate suspended particles of same size but different composition. Fluorescence based methods detects the fluorescence emission from aromatic components in the sample when it's irradiated with UV light. In this case the sensitivity is highly dependent on the relation between aromatics hydrocarbons and the rest of the oil components, while competing electronic decay processes and quenching alters the overall response at different concentration levels, thus introducing nonlinearities. Additionally some methods based on photoacustic sensors and UV/NIR light absorption were reported, but none has shown reliable at concentrations lower than 50 ppm.

Alternativelly, characterization methods based on thermal lens effects had been extensively developed since the first report of thermal lens effect by Gordon in 1965, leading to some of the most sensitive methods for thermophysical and chemical sample analysis methods, such as thermal lens spectroscopy. This technique is based on the measurement of the local refractive index variation that constitutes an optical lens induced by the light absorption and subsequent heating of an irradiated sample. Its application on chemical analysis is possible since the power of the lens depends on the concentration of absorbing components, hence allowing detection of absorbances as low as 10^{-7} AU. In comparison to other optical methods, thermal lens based techniques are intrinsically less sensitive to scattering effects, being ideal for characterization of heterogeneous samples or colloidal solutions, while also offering diverse and versatile configurations in order to exploit the photochemical properties of the sample. Thermal lens spectrometry has proven useful in diverse high sensitivity chemical trace detection and analysis, and it can also be coupled to chemical separation systems or microfluidic injection systems for enhanced selectivity.

In this work we present and discuss a novel water quality monitoring system for oil-in-water and suspended solids measurement based on thermal lens spectrometry and forward scattering. The device comprises a thermal lens spectrometer with a pump and probe beam configuration where both the power of the thermal lens and the optical transmission of the probe beam are measured. Transmission signal provides information about both absorbing (i.e. hydrocarbons) and scattering (i.e. suspended solids and oil droplets) components of the sample, while thermal lens signal only provides information about absorbing components. Thus, through signal processing it's possible to measure dissolved oil concentration as well as to detect oil droplets and suspended solids separately. Along our work the device was tested with water samples from both an injection well facility and a polymer manufacturing facility, and also with artificial colloidal solutions made for controlled tests. The whole system allowed a fast characterization of the sample with measurement durations of about 200 s, and since sample preparation isn't required and its configuration is compatible with a flow-through system, the device proves ideal for usage as an online monitor that can be incorporated in injection flowlines.

2. Experimental

The devices uses a thermal lens spectrometer configuration with two collineal beams, namely a high-power, intensity modulated pump beam and a low-power, non-modulated probe beam. The configuration consists of two main distinct sections: the thermal lens generation sector, which essentially comprises the lasers and the sample, and the focus error detection system through which the thermal lens power is measured. This allowed simultaneous measurement of both the thermal lens power and the optical transmission of the probe beam.

To generate the thermal lens, both beams are

focused on a sample contained in a flourometer cuvette. Along the beam propagation through the sample, the pump beam energy is partially absorbed and dissipated as heat, thus locally increasing the temperature of the medium and generating a refractive index profile. If the temperature elevation is smooth enough, the refractive index profile forms an optical element called a thermal lens that defocuses the probe beam due to the negative sign of the thermo-optic coefficient of water. In the low-absorption regime, the power of the thermal lens is proportional to the total energy absorbed, hence allowing to perform high-sensitivity absorbance measurements by characterizing the probe beam defocusing. Also, in order to achieve an efficient oil-in-water detection it's necessary to choose a pump wavelength that gives a high contrast between absorption from oil and water. Therefore we chose a 532 nm wavelength, at which the absorption coefficient of oil is typically 6 to 7 orders of magnitude larger than for water, and also high-power lasers are available.

Subsequently the probe beams enters the focus error detection system, where both the change of focus and its transmitted power are measured. The system comprises a pair of cylindrical lenses whose axes are oriented orthogonally, therefore creating an astigmatic focused beam with waists in the horizontal and vertical directions at different planes. There is an intermediate plane at which the beam is circular, and the presence of a thermal lens that defocuses the probe beam moves this plane along the optical axis. A four-quadrant photodiode was used to measure the beam ellipticity through generation of a focus error *FE* signal. Additionally, the total transmitted power is measured by summing the signals of all quadrants, enabling the usual measurement of the extinction coefficient through transmission. By normalizing *FE* with the transmitted power leads this signal to respond only to beam geometry independently of its intensity, and thus characterizing the probe beam defocusing: *FE* is zero when placed in the plane where the beam is circular, but in presence of a thermal lens, the beam on that plane becomes elliptical and leads to a nonzero *FE* signal.

Figure 1 shows a simplified diagram of the experimental setup. The sample was contained in a PMMA fluorometer cuvette with a 10 mm optical path. As a light source for the pump beam, we used a doubled Nd:YAG laser *Coherent* model *Compass 315M-100* with a 100 mW maximum output power at a 532 nm wavelength, and which was controlled by a driver provided by the manufacturer. The beam was then modulated by a chopper at a frequency of 350 Hz, which were much faster than the characteristic times of heat transfer by convection and diffusion processes, hence simplifying the thermal lens dependence by neglecting these effects. For the probe beam, a fiber-coupled laser diode *QPhotonics* model *QFLD-780-100S* was used, which provided a high quality gaussian beam with nearly 500 µW power on the sample at a 780 nm wavelength.

The pump beam focusing optics was chosen to obtain a confocal parameter on the sample similar to the optical path of the cuvette. In order to minimize aberrations introduced by the edges of the thermal lens, the probe beam focusing optics was chosen to maximize the path length over which the probe beam was smaller than the pump beam. Altogether, this led to beam waists of 55 µm for the pump beam and of 33 µm for the probe beam. To control the displacement between both waists along the optical axis, the pump beam passed through a simple optical delay line comprised of two mirrors on a translation stage.

The focus error detection system comprised two 75 mm focal length cylindrical lenses and a 1 mm^2 total active area four-quadrant photodetector. The system has two free parameters, namely the separation between the lenses and the distance from the lenses to the sample, which were chosen in order to optimize the sensitivity of the *FE* signal in the presence of a thermal lens. To do so, the beam propagation and the *FE* signal were simulated as a function of those parameters, and the optimal configuration within the mechanical limitations was chosen. Afterwards, the detector was positioned on the plane where the probe beam was circular. In practice, the focus error signal was obtained from a series of summing op-

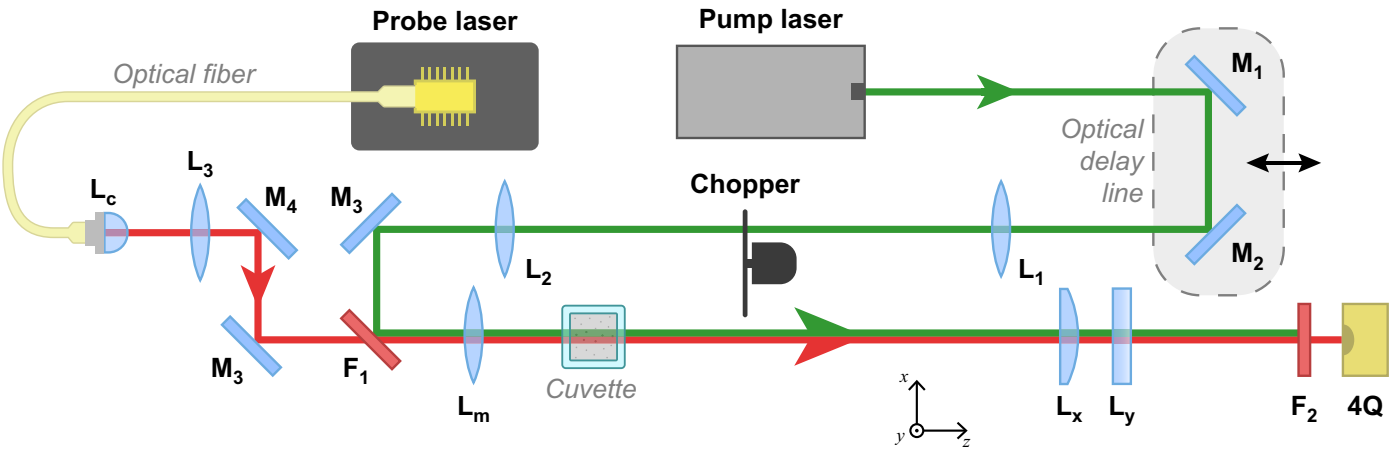

Figure 1: Experimental setup. **M_1 to M_5:** mirrors for beam alignment. **L_c:** probe collimating lens. **L_1 to L_3:** pump and probe optics, in addition with **L_m**. **F_1 and F_2:** 700 nm longpass filter for beam coupling and pump filtering respectively. **L_x and L_y:** cylindrical lenses. **4Q:** four-quadrant photodiode.

amps circuits and then it was acquired and processed by a 1 MHz bandwidth, PCI lock-in amplifier *Anfatec* model *AMU 2.4*, in order to filter the harmonic component at the pump modulation frequency by connecting the phase-locked loop input to the chopper reference output. Additionally, the signal from each quadrant was acquired by a 16 bits, 1 MHz bandwidth, PCI DAQ *IOtech* model *DaqBoard/3001*. This allowed to measure the total transmitted power by summing the signals from all quadrants through software and hence to normalize *FE* signal, and also to generate additional auxiliary signals.

With our prior understanding of the system we can already anticipate the signals responses in the presence of a sample of oil-in-water. On the one hand, the absorbing components dissolved in water along with water itself will contribute to generate a thermal lens distributed over the irradiated volume, therefore increasing the thermal lens channel level and decreasing the transmission channel level due to light extinction. On the other hand, suspended particles such as solids or oil droplets will also pass through the beams. If the particle does not absorbs the pump radiation, it will act as a scattering center and decrease the transmitted power, which will be observed as a negative peak on transmission channel. If the particle does absorb the pump radiation, in addition to light scattering it will generate a thermal lens located around itself and thus defocusing the probe beam even more, which will be observed as an additional positive peak in the thermal lens channel. To extract the thermal lens power from dissolved components we compute the mode of the normalized thermal lens signal, which gives the absorption base level from the sample. To detect the suspended particles we use a peak detection algorithm developed on *Matlab* that compares the signal fluctuations with those obtained on a pure demineralized sample. In our work, these two measurements were performed in an post-processing stage, but they also can be conducted on real-time processing.

Our experiments were designed and conducted to study the system behavior considering the above discussed preliminar analysis. For this, we have two master samples taken from an injection well facility located in Comodoro Rivadavia, Argentina. The first one, which we will refer as IW100, is a sample of the injection water that consists on treated produced water, and had oil-in-water concentration of at least 100 ppm. The second one, which we will refer as IW10, is a sample of the water used for polymer manufacturing that consists on the same injection water with further treatment, and had a oil concentration lesser than 10 ppm. The concentration values were given by the company that took the samples and performs

water quality analysis periodically on this well. Additionally, to study the system behavior when analyzing the suspended particles with controlled samples, we prepared artificial samples from solutions of microspheres on demineralized water. To simulate scattering centers we used polystirene spheres with a diameter of 6 µm, while to simulate absorption centers we used polystirene spheres dyed with a red pigment (thus absorbing at a 532 nm wavelength) with diameters of 6 µm and 2 µm. We will refer to each master sample made as PS6 for the 6 µm diameter undyed polystirene spheres, and as PSD6 and PSD2 for the 6 µm diameter and 2 µm diameter respectively polystirene dyed spheres. All spheres were manufactured by *Phosphorex Inc.*

3. Results and discussion

To study the system capacity for characterizing dissolved components we performed serial dilutions of the IW100 and IW10 samples. First we progressively diluted IW100 on IW10, thus varying the oil concentration while preserving some of the water components. Secondly we diluted IW10 on demineralized water to extend the concentration range to lower values. For each iteration we performed a measurement with the same fixed parameters, namely lasers output power, acquisition length, lock-in and DAQ parameters, etc., and then processed the data as mentioned above obtaining the results plotted in figure 2

The measurements for dilutions of IW10 on water allowed to study the performance of the device for injection water samples in the lowest absorption regime, recovering a linear response over the whole range of concentrations. A least squares linear regression was performed on the data, and from the adjusted slope it was possible to experimentally estimate the sensitivity of the device in therms of concentration by assuming an oil concentration of 10 ppm for the pure IW10 sample, resulting in a sensitivity of $(1.8084 \pm 0.0034) \times 10^{-5}\,\mathrm{ppm}^{-1}$ (note that *FE* has no units after normalization with the transmission signal). If the actual concentration of the master sample would be lower, our sensitivity would rise, and therefore this value corresponds to a lower bound for the device sensitivity on these samples.

The ability to detect a certain amount of oil in the sample corresponds to the ability to distinguish its signal level from the background signal due to absorption of water. Resolution is thus limited by the signal fluctuations, which mainly includes the noise of the system and the inhomogeneities in the sample composition, and varies with the time constant of the lock-in amplifier and the total acquisition duration. Dependence with time constant is trivial since a bandwidth reduction leads to an integration over a larger time window, thus reducing the signal fluctuations. Unlike this, dependence of a measurement uncertainty with the acquisition duration is more complex and improves with a better reconstruction of the signal distribution since we are estimating the signal mode, which is an statistical variable. By measuring the mode variance of a IW100 sample as a function of the acquisition length we observed that this dispersion diminished approximately 8 times for lengths up to 200 s and remained constant for larger values. Therefore we take the resolution of the device as the minimum distinguishable concentration for this acquisition lengths, and we do so independently of the sample by taking account only for fluctuations introduced by the system noise (i.e. without sample), obtaining a resolution of 0.02 ppm with the acquisition parameters used on our measurements.

Additionally, the dilutions of IW100 in IW10 allowed us to cover the range of concentrations of interest for injection and polymer manufacturing purposes. In this case it was necessary to correct the signal levels due to degradation of the samples caused by the large time of exposure to light radiation. It should be mentioned that this effect was significant because the serial dilution protocol used spanned through several hours, but otherwise negligible in each iteration, for measurements of durations lesser than 20 min or in an online operation. After corrections, we again observed a linear response that gives the calibration coefficients for this well once the exact oil concentration of the master samples are known. In all cases the measurement precision (obtained

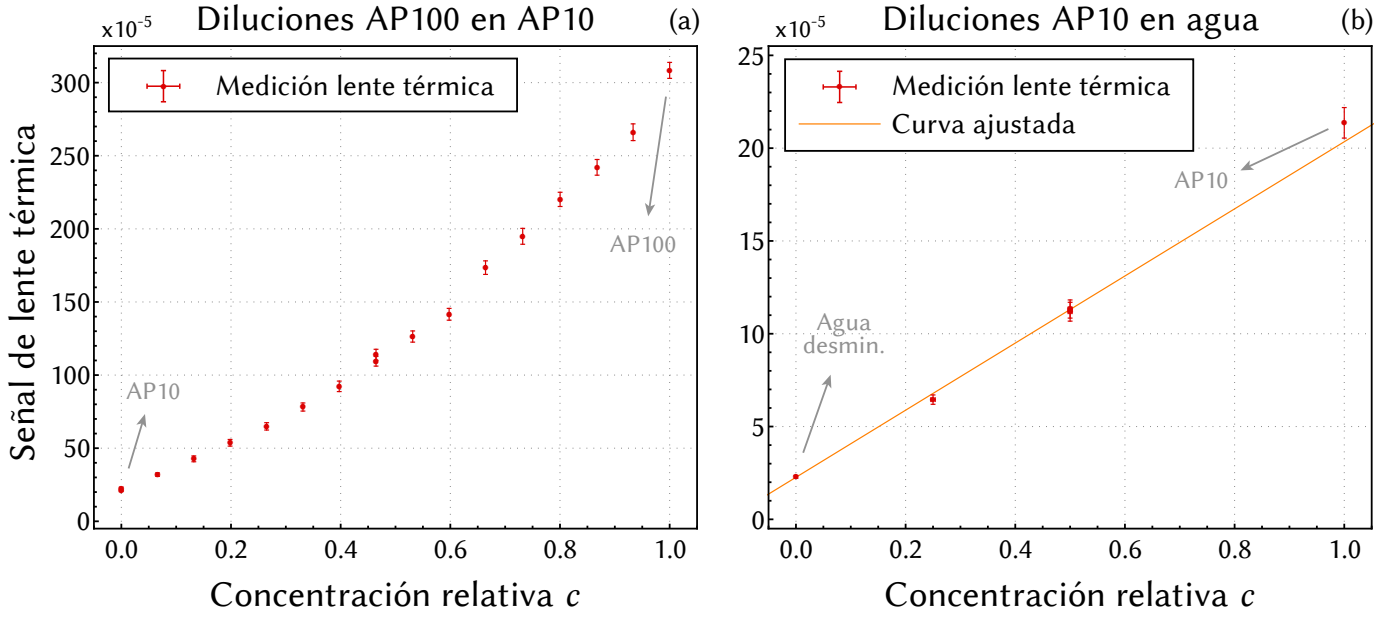

Figure 2: Thermal lens signal from bulk absorption of dissolved components for serial dilutions of (a) IW100 on IW10 and (b) IW10 on demineralized water.

by taking account for all fluctuations) was better than 5 %, being mostly limited by the fluctuations introduced by the sample inhomogeneous composition. Hence after proper calibration, an oil concentration around 30 ppm could be determined with an error lesser than 0.6 ppm.

When studying the system capacity for particles and emulsion characterization, we initially observed that the time series acquired for solutions of spheres in water agreed with the expected behavior of the signals described in our preliminary analysis. To do so, firstly the amount of peaks registered for each solution was calculated and compared with a pure water reference. The undyed spheres, which acted as scattering centers, showed a relevant increase of negative peaks in the transmission channel, where approximately 40 times more negative peaks were detected. Also we didn't register an increase in peaks for the thermal lens channel, indicating not only the absence of absorption centers but also that the thermal lens signal is not affected by scattering losses. Additionally, the dyed spheres showed a similar increase for both negative peaks in the transmission channel and positive peaks in the thermal lens channel, indicating the spheres acted as both scattering and absorption centers.

To study the magnitude of the effects introduced by particles, we compute the height p of each peak relative to the base signal level due to the bulk absorption of the sample. Figure 3 shows an histogram of the peak relative heights for all samples registered at (a) the transmission channel and (b) the thermal lens channel. When comparing particles of different sizes, the negative peaks in transmission channel reveals that larger spheres produces a distribution of higher peaks. This is also shown by the calculated mean peak height, which was of 19.9×10^{-3} for PS6 sample and of 17.5×10^{-3} for PS2 sample (absolute values of 0.422 V and 0.404 V respectively), while the PSD2 sample had a mean height of 6.54×10^{-3} (absolute height of 0.140 V). As expected, there isn't any significant difference between the distributions for spheres of the same size in this channel, whether dyed or undyed, indicating that absorption losses are negligible in relation to the total incident power.

From figure 3 (b) we can make a similar analysis regarding the thermal lens channel, where we excluded the PS6 sample since it didn't pro-

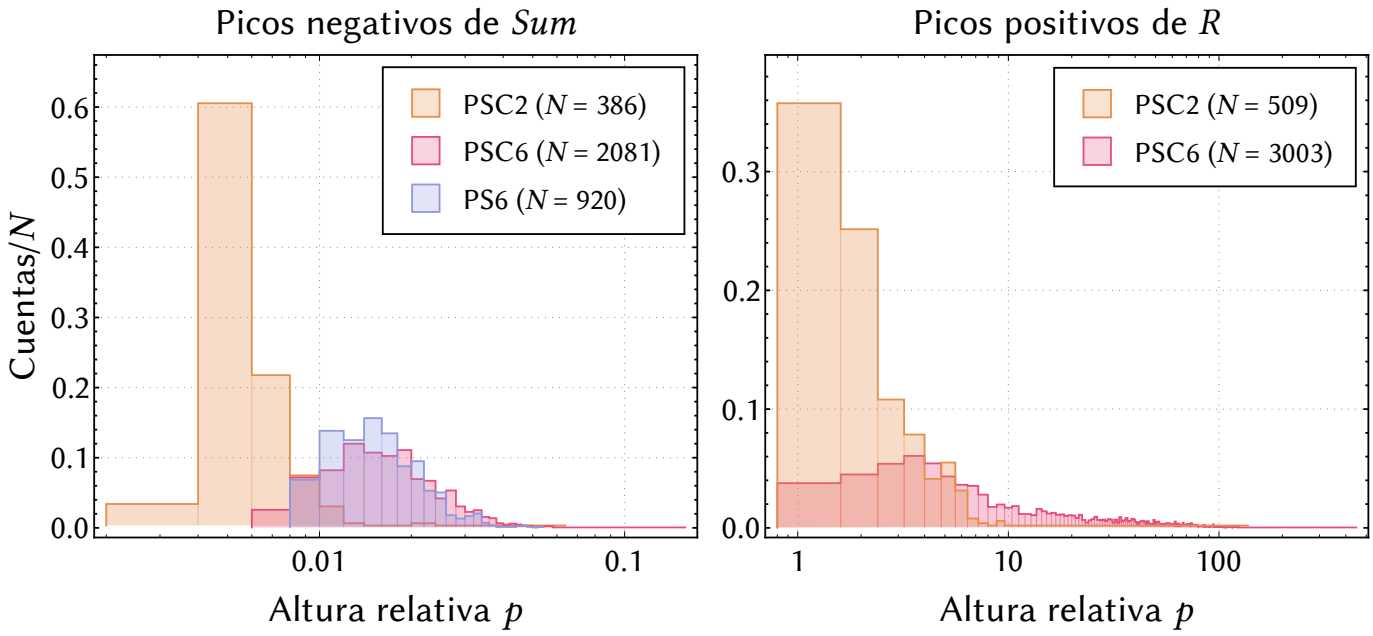

Figure 3: Histogram of relative peaks heights for (a) transmission channel and (b) thermal lens channel. On each case, counts are normalized to the total number of peaks detected N.

duce a significant amount of peaks on this signal. Here again we observe a distribution of peaks with larger heights for the solution with bigger spheres, which is also consistent with the calculated mean peak heights of 24.8 for PSD6 sample and 2.86 for PSD2 sample (absolute heights of 7.74×10^{-4} and 1.00×10^{-4} respectively). Considering that the thermal lens channel is insensitive to scattering from a single particle, the information provided by both channels is complementary and allows to differentiate between particles by their absorption and scattering properties in therms of size and pigmentation, since the peak heights correlates with their scattering or absorption cross section depending on the channel. It should be noted that peak detection is much more improved on the thermal lens channel, where typical peak relative heights are several orders of magnitude larger than in transmission channel. This is due to both the better signal-to-noise ratio in phase-sensitive detection and the choice for a pump wavelength in the water absorption minimum, resulting in a higher contrast on the signal and therefore an efficient peak detection that enhances characterization of the absorbing components in the sample.

In order to study the frequency of peaks, we calculated the interarrival time Δ between particles passing through the beams. Assuming a solution of ideal and statistically independent particles and for concentrations low enough to consider the probability of finding one particle in the sample volume negligible, the passage of particles through the beams follows a Poisson distribution in which interarrival times have a probability distribution

$$P(\Delta > t) = \exp(-bt), \tag{1}$$

with b being the reciprocal mean interarrival time, i.e. $\langle\Delta\rangle = 1/b$. We verified this behavior by computing the cumulative distribution probability of Δ for both the negative peaks of transmission channel and positive peaks of thermal lens channel, obtaining a probability distribution that agrees with 1 for values of Δ greater than minimum interarrival time Δ_{min} our system could resolve. Here, Δ_{min} was limited mainly by the average peak width, the time constant of the lock-in amplifier and the fact that our system can't distinguish between one or many particles in the sample volume.

Under previous assumptions, it's fairly simple to derive from first principles an expression for

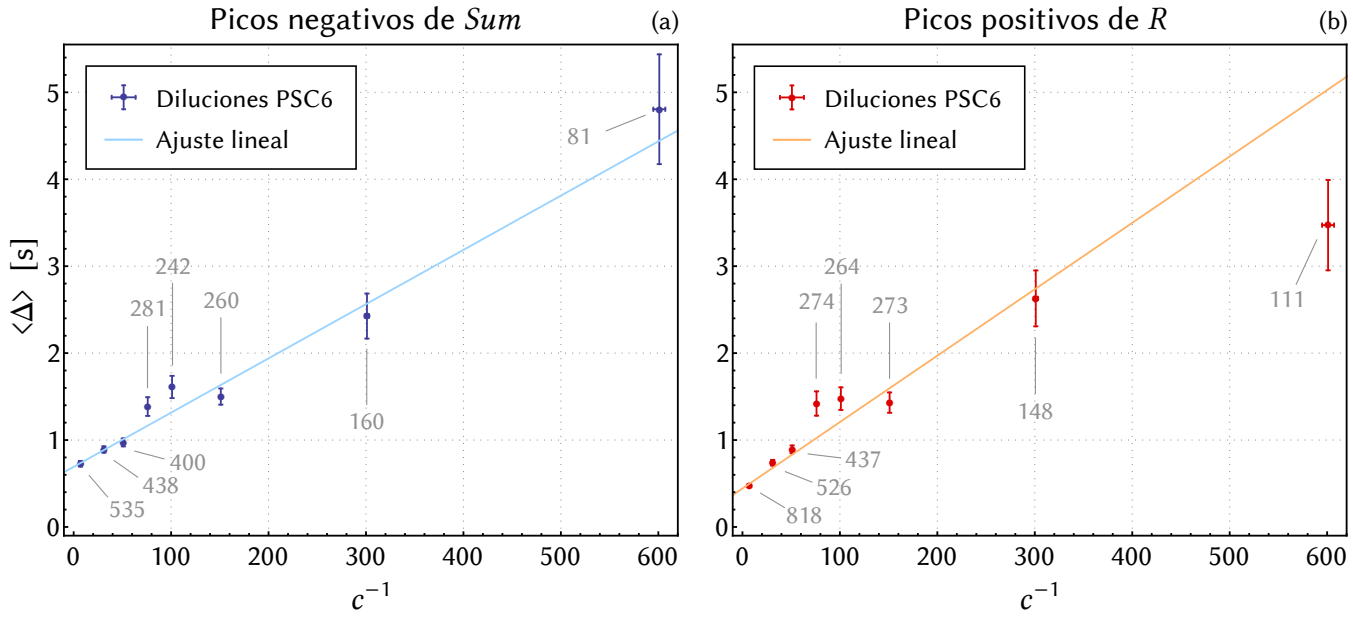

Figure 4: Mean interarrival times of (a) peaks on transmission channel and (b) peaks on thermal lens channel obtained for serial dilutions of PS6 on demineralized water, plotted against the reciprocal relative concentration c. Along with data points, the number of peaks detected for each dilution is indicated.

the parameter b, obtaining

$$b = 2w_0 l u_\perp C, \tag{2}$$

where l is the optical path of the cuvette, $2w_0$ is the beam diameter, $u_\perp$ is the mean flow velocity in the direction transverse to the optical axis and C is the particle concentration. Hence 2 corresponds to the flow of particles through the sampling volume. It should be mentioned that this expression is valid for a collimated beam in a uniform transverse flow, but it could be extended for focused beams and an almost arbitrary flow by considering an effective sample volume and a mean transverse flow velocity. Thus, by knowing the sampling volume and the particle speed, the concentration C can be estimated from the mean interarrival time $\langle\Delta\rangle$.

Consequently we performed an acquisition for a serial dilution of all master samples in water and measured $\langle\Delta\rangle$ for each iteration. Figure 4 shows the values of $\langle\Delta\rangle$ plotted against the reciprocal relative concentration c^{-1} of each solution for dilutions of the PSD6 master sample, indicating alongside the amounts of events detected on each iteration. We recall that for these experiments, the flow velocity was determined only by flow convection due to heat dissipation, thus varying for different concentrations since the amount of absorbed energy changed. Nevertheless, for both channels we observed a linear trend which we verified with a weighted linear regression. The adjusted slope is then associated to the sensitivity of our method, while the y-intercept is associated to Δ_{min} and limits our dynamic range, since it corresponds to concentrations where the probability to find more than one particle in the beam is significant. Therefore by knowing the exact concentrations of each solutions it is possible to obtain calibrations coefficients from the linear regression to finally measure absolute concentrations of absorbing and non-absorbing particles independently. For this purpose, a linear, homogeneous and controlled flow profile (as it would be obtained with a proper installation of the system on the injection flowline) would be best suited since it provides a well-defined particle speed and allows to tune the acquisition parameters to maximize the detection range and sensitivity.

4. Conclusions